Hadronic contribution from light by light processes in (g-2) of muon in nonlocal quark model.*

A. S. Zhevlakov[1;1)] A. E. Dorokhov[2;2)] A. E. Radzhabov[3;3)]

[1] Department of Physics, Tomsk State University, Lenin ave. 36, 634050 Tomsk, Russia
[2] Bogoliubov Laboratory of Theoretical Physics, JINR, 141980 Dubna, Russia
[3] 3 Institute for System Dynamics and Control Theory SB RAS, 664033 Irkutsk, Russia

Abstract: The hadronic corrections to the muon anomalous magnetic moment a_μ, due to the full gauge-invariant set of diagrams with dynamical quark loop and intermediate pseudoscalar and scalar states light-by-light scattering insertions, are calculated in the framework of the nonlocal chiral quark model. These diagrams correspond to all hadronic light-by-light scattering contributions to a_μ in the leading order of the $1/N_c$ expansion in quark model. The result for the quark loop contribution is $a_\mu^{\rm HLbL,Loop} = (11.0 \pm 0.9) \cdot 10^{-10}$, and the total result is $a_\mu^{\rm HLbL,N\chi QM} = (16.8 \pm 1.2) \cdot 10^{-10}$.

Key words: anomalous magnetic moment of muon, nonlocal model, light-by-light, chiral model

PACS: 12.39.Fe, 13.40.Em

1 Introduction

The anomalous magnetic moment (AMM) of lepton and contribution of light by light (LbL) processes has a long history of investigation. After latest experiment on measurement of AMM of muon in BNL E821 [1] the interest to this topic are return. Two new experiments on measurement of AMM of muon are under construction in Fermilab [2] and J-PARC [3, 4]. New precision data are demand more accurate calculations.

The most problematic part of the calculation AMM of muon is segment associated with the strong interaction because most of this contribution is in nonperturbative low energy region. This contribution consist of hadron vacuum polarization (HVP) part (leading in α) and LbL scattering through the nonperturbative QCD vacuum (sub-leading in α). The HVP contribution can be extracted from the experimental data but the contribution of LbL scattering needs to be modeled.

What degrees of freedom (DoF) are relevant for modeling of strong interaction at low energy: mesons or quarks (and gluons)? This question is connected with confinement problem and is one of the most important tasks in physics of strong interaction. One can separate two different approaches for description of LbL processes. In first one the only mesonic DoF are used. The second one starts from quark Lagrangian and have mesonic DoF as a bound states.

2 Model

The LbL contribution to AMM of muon is in low energy region where the perturbative methods of QCD are not applicable.

Nonlocal quark model NχQM is nonlinear realization of Nambu-Jona-Lasinio model. Nonlocality can be motivated by instanton liquid model. The model is formulated in terms of quark degrees of freedom and bound states corresponds to mesons. The circumscribing of model is made in works [5, 6] and here we give brief description model properties that is needed for calculation of AMM.

2.1 Lagrangian

The Lagrangian of the SU(3) nonlocal chiral quark model with the SU(3)×SU(3) symmetry has the form

$$\mathcal{L} = \bar{q}(x)(i\hat{\partial} - m_c)q(x) + \frac{G}{2}[J_S^a(x)J_S^a(x) + J_{PS}^a(x)J_{PS}^a(x)] - \frac{H}{4}T_{abc}\Big[J_S^a(x)J_S^b(x)J_S^c(x) - 3J_S^a(x)J_{PS}^b(x)J_{PS}^c(x)\Big], \quad (1)$$

where $q(x)$ are the quark fields, m_c ($m_u = m_d \neq m_s$) is the diagonal matrix of the quark current masses, G and H are the four- and six-quark coupling constants. Second line in the Lagrangian represents the Kobayashi–Maskawa–t'Hooft determinant vertex with the structural

Received 20 Nov. 2015
* The work is supported by Russian Science Foundation Grant (RSCF 15-12-10009)
1) E-mail: zhevlakov@phys.tsu.ru
2) E-mail: dorokhov@theor.jinr.ru
3) E-mail: aradzh@icc.ru

constant

$$T_{abc} = \frac{1}{6}\epsilon_{ijk}\epsilon_{mnl}(\lambda_a)_{im}(\lambda_b)_{jn}(\lambda_c)_{kl}, \quad (2)$$

where λ_a are the Gell-Mann matrices for $a = 1,..,8$ and $\lambda_0 = \sqrt{2/3}I$.

The nonlocal structure of the model is introduced via the nonlocal quark currents

$$J^a_M(x) = \int d^4x_1 d^4x_2\, f(x_1)f(x_2)\,\bar{q}(x-x_1)\Gamma^a_M q(x+x_2), \quad (3)$$

where $M = S$ for the scalar and $M = PS$ for the pseudoscalar channels, $\Gamma^a_S = \lambda^a$, $\Gamma^a_{PS} = i\gamma^5\lambda^a$ and $f(x)$ is a form factor with the nonlocality parameter Λ reflecting the nonlocal properties of the QCD vacuum.

The model can be bosonized using the stationary phase approximation which leads to the system of gap equations for the dynamical quark masses $m_{d,i}$

$$m_{d,i} + GS_i + \frac{H}{2}S_jS_k = 0, \quad (4)$$

with $i = u,d,s$ and $j,k \neq i$, and S_i is the quark loop integral

$$S_i = -8N_c \int \frac{d^4_E k}{(2\pi)^4}\frac{f^2(k^2)m_i(k^2)}{D_i(k^2)},$$

where $m_i(k^2) = m_{c,i} + m_{d,i}f^2(k^2)$, $D_i(k^2) = k^2 + m_i^2(k^2)$ is the dynamical quark propagator obtained by solving the Dyson-Schwinger equation, $f(k^2)$ is the nonlocal form factor in the momentum representation. For calculation was used two different form-factors: Gaussian form

$$f(p^2) = \exp\left(-\frac{p^2}{2\Lambda^2}\right) \quad (5)$$

monopole form

$$f(p^2) = \left(1 + \frac{p^2}{\Lambda^2}\right)^{-1} \quad (6)$$

where Λ is cutoff parameter. The model have five parameters which can fitted on physical observables. In order to investigate the sensitivity of model to the changing of model parameters the dynamical mass of light quark is varying between 200-350 MeV with corresponding refit of other parameters. This region corresponds to the more or less physical range of dynamical quark mass.

2.2 Meson propagator

The quark-meson vertex functions and the meson masses can be found from the solution of Bethe-Salpeter equation Fig. 1. For the separable interaction [6] the quark-antiquark scattering matrix in each (PS or S) channels becomes

$$\mathbf{T} = \hat{\mathbf{T}}(p^2)\delta^4(p_1+p_2-(p_3+p_4))\prod_{i=1}^{4} f(p_i^2),$$
$$\hat{\mathbf{T}}(p^2) = i\gamma_5\lambda_k\left(\frac{1}{-\mathbf{G}^{-1}+\mathbf{\Pi}(p^2)}\right)_{kl} i\gamma_5\lambda_l, \quad (7)$$

where p_i are the momenta of external quark lines, $\mathbf{G}$ and $\mathbf{\Pi}(p^2)$ are the corresponding matrices of the four-quark coupling constants and the polarization operators of mesons ($p = p_1 + p_2 = p_3 + p_4$). The meson masses can be found from the zeros of determinant $\det(\mathbf{G}^{-1} - \mathbf{\Pi}(-M^2)) = 0$. The $\hat{\mathbf{T}}$-matrix for the system of mesons in each neutral channel can be expressed as

$$\hat{\mathbf{T}}_{ch}(P^2) = \sum_{M_{ch}} \frac{\overline{V}_{M_{ch}}(P^2)\otimes V_{M_{ch}}(P^2)}{-(P^2+\mathrm{M}^2_{M_{ch}})}, \quad (8)$$

where M_M are the meson masses, $V_M(P^2)$ are the vertex functions $\left(\overline{V}_M(p^2) = \gamma^0 V^\dagger_M(P^2)\gamma^0\right)$. The sum in (8) is over full set of light mesons: $(M_{PS} = \pi^0, \eta, \eta')$ in the pseudoscalar channel and $(M_S = a_0(980), f_0(980), \sigma)$ in the scalar one.

Details about vertex of interaction of mesons with quarks, meson propagator, etc. mixing can be found in [5, 7, 8].

2.3 Interaction with external photons

The bext step for description LbL processes is to introduce in the nonlocal chiral Lagrangian (1) the gauge-invariant interaction with an external photon field $A_\mu(z)$ by Schwinger factor (9). In result we obtain infinite series of vertexes quark-antiquark interactions with photons.

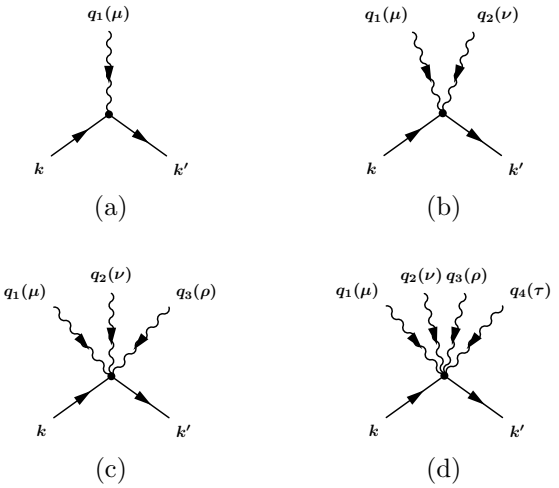

Fig. 2. The quark-photon vertex $\Gamma^{(1)}_\mu(q)$, the quark-two-photon vertex $\Gamma^{(2)}_{\mu\nu}(q_1,q_2)$, the quark-three-photon vertex $\Gamma^{(3)}_{\mu\nu\rho}(q_1,q_2,q_3)$, and the quark-four-photon vertex $\Gamma^{(4)}_{\mu\nu\rho\tau}(q_1,q_2,q_3,q_4)$.

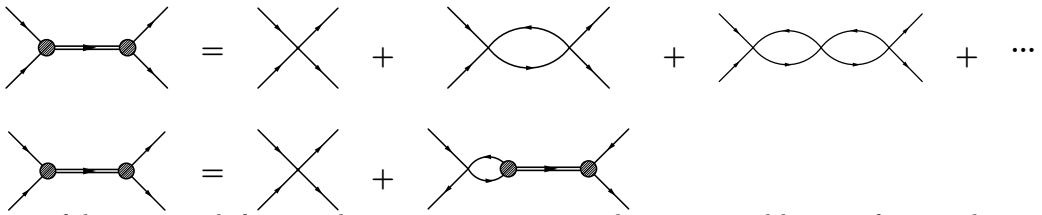

Fig. 1. The set of diagrams with four-quarks interaction vertex can be represented by pure four-quark vertex and sum of diagram that will associated with meson exchange.

$$q(y)\to Q(x,y)=\mathcal{P}\exp\left\{i\int_x^y dz^\mu A_\mu(z)\right\}q(y). \qquad (9)$$

The scheme, based on the rules that the derivative of the contour integral does not depend on the path shape

$$\frac{\partial}{\partial y^\mu}\int_x^y dz^\nu\ F_\nu(z)=F_\mu(y),\quad \delta^{(4)}(x-y)\int_x^y dz^\nu\ F_\nu(z)=0,$$

was suggested in [9] and applied to nonlocal models in [10]. The actual form of the vertexes shown in Fig. 2 can be found in [11].

2.4 Box diagram

In effective quark model under consideration there are two different parts which corresponds to contact contribution or contribution with intermediate meson.

Using quark-antiquark interactions vertexes with one, two, three of four photons, see Fig. 2, we can build five types of diagrams.

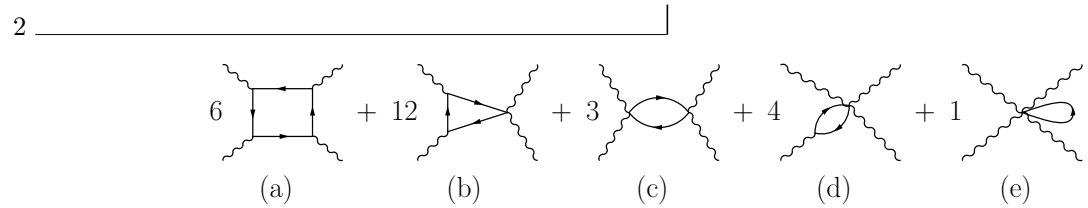

Fig. 3. The box diagram and the diagrams with nonlocal multiphoton interaction vertices that give the contributions to $\Pi_{\mu\nu\lambda\rho}(q_1,q_2,q_3)$. The numbers in front of the diagrams are the combinatoric factors.

Only the sum of all diagrams is gauge invariant and is correspond to contact (or quark loop) contribution.

3 LbL in AMM of muon

The contribution of light by light process to AMM of muon has the form:

$$a_\mu^{\rm LbL}=\frac{e^6}{48m_\mu}\int\frac{d^4q_1}{(2\pi)^4}\int\frac{d^4q_2}{(2\pi)^4}\times \\ \times\frac{\Pi_{\rho\mu\nu\lambda\sigma}(q_2,-q_3,q_1)\mathrm{T}^{\rho\mu\nu\lambda\sigma}(q_1,q_2,p)}{q_1^2q_2^2q_3^2((p+q_1)^2-m_\mu^2)((p-q_2)^2-m_\mu^2)}, \qquad (10)$$

where the tensor $\mathrm{T}^{\rho\mu\nu\lambda\sigma}$ is the Dirac trace

$$\mathrm{T}^{\rho\mu\nu\lambda\sigma}(q_1,q_2,p)=\mathrm{Tr}\Big((\hat p+m_\mu)[\gamma^\rho,\gamma^\sigma](\hat p+m_\mu)\times \\ \times\gamma^\mu(\hat p-\hat q_2+m_\mu)\gamma^\nu(\hat p+\hat q_1+m_\mu)\gamma^\lambda\Big).$$

Taking the Dirac trace, the tensor $\mathrm{T}^{\rho\mu\nu\lambda\sigma}$ becomes a polynomial in the momenta p, q_1, q_2.

After that, it is convenient to convert all momenta into the Euclidean space, and we will use the capital letters P, Q_1, Q_2 for the corresponding counterparts of the Minkowskian vectors p, q_1, q_2, e.g. $P^2=-p^2=-m_\mu^2$,

*The possible combinations with momentum P are

$$(P\cdot Q_1)^2=(P\cdot Q_1)(D_1-Q_1^2)/2,\quad (P\cdot Q_2)^2=-(P\cdot Q_2)(D_2-Q_2^2)/2,$$
$$(P\cdot Q_1)(P\cdot Q_2)=-(D_1-Q_1^2)(D_2-Q_2^2)/4,$$
$$(P\cdot Q_1)=(D_1-Q_1^2)/2,\quad (P\cdot Q_2)=-(D_2-Q_2^2)/2.$$

$Q_1^2=-q_1^2$, $Q_2^2=-q_2^2$. Then Eq. (10) becomes

$$a_\mu^{\rm LbL}=\frac{e^6}{48m_\mu}\int\frac{d_E^4Q_1}{(2\pi)^4}\int\frac{d_E^4Q_2}{(2\pi)^4}\frac{1}{Q_1^2Q_2^2Q_3^2}\frac{{\rm T}^{\rho\mu\nu\lambda\sigma}\Pi_{\rho\mu\nu\lambda\sigma}}{D_1D_2},$$
$$D_1=(P+Q_1)^2+m_\mu^2=2(P\cdot Q_1)+Q_1^2,x \qquad (11)$$
$$D_2=(P-Q_2)^2+m_\mu^2=-2(P\cdot Q_2)+Q_2^2.$$

Since the highest order of the power of the muon momentum P in ${\rm T}^{\rho\mu\nu\lambda\sigma}$ is two * and $\Pi_{\rho\mu\nu\lambda\sigma}$ is independent of P, the factors in the integrand of (11) can be rewritten as

$$\frac{{\rm T}^{\rho\mu\nu\lambda\sigma}\Pi_{\rho\mu\nu\lambda\sigma}}{D_1D_2}=\sum_{a=1}^{6}A_a\tilde{\Pi}_a, \qquad (12)$$

with the coefficients

$$A_1=\frac{1}{D_1},\quad A_2=\frac{1}{D_2},\quad A_3=\frac{(P\cdot Q_2)}{D_1},\quad A_4=\frac{(P\cdot Q_1)}{D_2},$$
$$A_5=\frac{1}{D_1D_2},\quad A_6=1, \qquad (13)$$

where all P-dependence is included in the A_a factors, while $\tilde{\Pi}_a$ are P-independent.

Then, one can average over the direction of the muon momentum P (as was suggested in [12] for the pion-exchange contribution)

$$\int\frac{d_E^4Q_1}{(2\pi)^4}\int\frac{d_E^4Q_2}{(2\pi)^4}\frac{A_a}{Q_1^2Q_2^2Q_3^2}...=$$
$$\frac{1}{2\pi^2}\int_0^\infty dQ_1\int_0^\infty dQ_2\int_{-1}^{1}dt\sqrt{1-t^2}\frac{Q_1Q_2}{Q_3^2}\langle A_a\rangle..., \qquad (14)$$

where the radial variables of integration $Q_1\equiv|Q_1|$ and $Q_2\equiv|Q_2|$ and the angular variable $t=(Q_1\cdot Q_2)/(|Q_1||Q_2|)$ are introduced. The averaged A_a factors was introduced in [12]

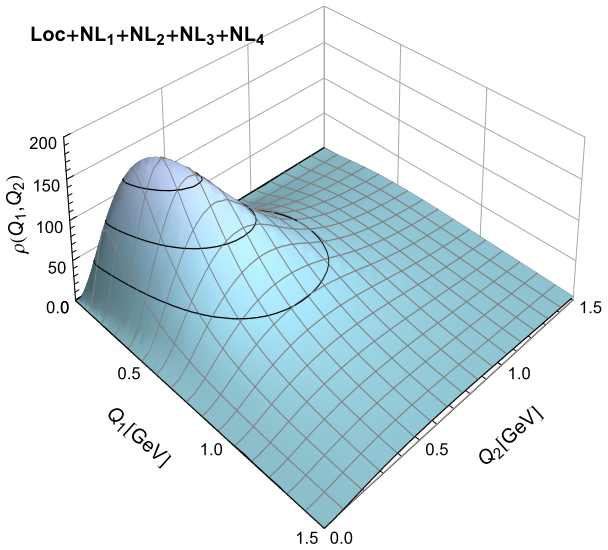

Fig. 4. The 3D density $\rho(Q_1,Q_2)$ defined in Eq. (15).

3.1 Density function

For investigation of the dependence of contribution from photon legs virtuality one can watch for "density function". This is the function which corresponds to the LbL contribution to AMM before integration over intermediate photons virtualities.

$$\rho^{\rm LbL}(Q_1,Q_2)=\frac{Q_1Q_2}{2\pi^2}\sum_{a=1}^{6}\int_{-1}^{1}dt\,\frac{\sqrt{1-t^2}}{Q_3^2}\langle A_a\rangle\tilde{\Pi}_a. \qquad (15)$$

The volume under 3D -density function is full contribution to AMM of muon. In Fig. 5 this function is shown for nonlocal model in leading $1/N_c$ order.

One can see that contribution is mainly localized in a range of virtualities of photons around 1 GeV.

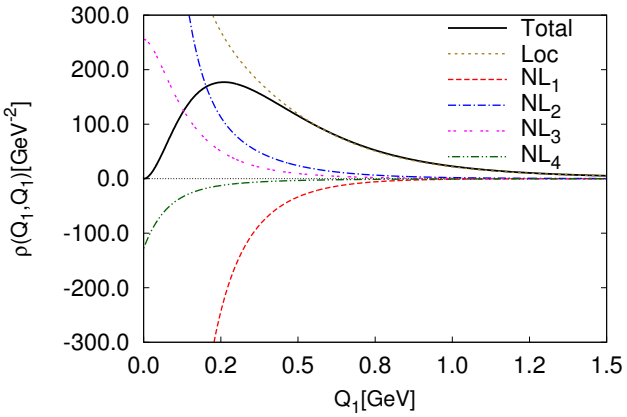

Fig. 5. The 2D slice of the density $\rho(Q_1,Q_2)$ at $Q_2=Q_1$. Different curves correspond to the contributions of topologically different sets of diagrams drawn in Fig. 3. The contribution of the box diagram with the local vertices, Fig. 3a, is the dot (olive) line(Loc); the box diagram, Fig. 3a, with the nonlocal parts of the vertices is the dash (red) line (NL_1); the triangle, Fig. 3b, and loop, Fig. 3c, diagrams with the two-photon vertices is the dash-dot (blue) line (NL_2); the loop with the three-photon vertex, Fig. 3d, is the dot-dot (magenta) line (NL_3); the loop with the four-photon vertex, Fig. 3e, is the dash-dot-dot (green) line (NL_4); the sum of all contributions (Total) is the solid (black) line. At zero all contributions are finite.

In Fig. 5, the slice of $\rho^{\rm HLbL}(Q_1,Q_2)$ in the diagonal direction $Q_2=Q_1$ is presented together with the partial contributions from the diagrams of different topology. One can see, that the $\rho^{\rm HLbL}(0,0)=0$ is due to a nontrivial cancellation of different diagrams of Fig. 3. This important result is a consequence of gauge invariance and the spontaneous violation of the chiral symmetry, and represents the low energy theorem analogous to the theorem for the Adler function at zero momentum. Another interesting feature is, that the large Q_1, Q_2 behavior is dominated by the box diagram with local vertices and quark propagators with momentum-independent masses in accordance with perturbative theory. All this is very important characteristics of the NχQM, interpolating the well-known results of the chiral perturbative theory at low momenta and the operator product expansion at large momenta. Earlier, similar results were obtained for the two-point [13] and three-point [14] correlators.

4 Results and conclusion

The contribution to AMM of muon from LbL process in NχQM correspond contributions from contact term and term with intermediate pseudoscalar and scalar channels. The contact term contribution is:

$$a_\mu^{\rm HLbL,Loop}=(11.0\pm0.9)\cdot10^{-10}. \qquad (16)$$

And the total contribution is estimated as

$$a_\mu^{\rm HLbL}=16.8(1.25)\cdot10^{-10}, \qquad (17)$$

where error bar is the band in region of physical dynamical mass.

In Fig. 6 one can see that it is important, at least in the framework of quark model, to take into account not only diagrams with intermediate mesons but also the contact term (or quark loop) contribution.

In comparison with other model calculation, our results are quite close to the recent results obtained in [15, 16]. The specific feature of our model and Dyson-Schwinger approach [15] is that the due to nonlocal interaction kernel the quarks becomes dynamical one with momentum-dependent mass. The predictions of the NχQM for the different contributions to the muon $g-2$ are in agreement with [15] within 10%.

The next step of calculations is to extend quark model in order to estimate subleading in $1/N_c$ terms. This subleading contribution from diagrams with meson loop has negative sign [17].

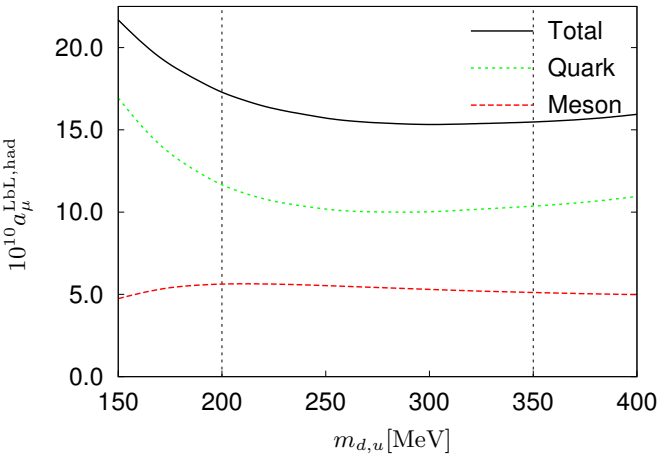

Fig. 6. The contribution of muon AMM from LbL depending on the dynamical mass of quark $m_{d,u}$ in zero order on $1/N_c$. The solid curve is total contribution, red and green dashed curve — contact terms Fig. 3 and meson exchange [7, 8] respectively.

For solving the puzzle of LbL contribution, we should to better understanding the physics of strong interaction at long distance. In principle one can do this with more accurate measurement of meson form factors.

References

1 G.W. Bennett, et al. [Muon (g-2) Collaboration], Phys.Rev. **D73**, 072003 (2006).
2 G. Venanzoni [Fermilab E989 Collaboration], J. Phys. Conf. Ser. **349** (2012) 012008. E989 experiment at Fermilab: http://gm2.fnal.gov/
3 N. Saito [J-PARC g-2/EDM Collaboration], AIP Conf. Proc. **1467**, 45 (2012).
4 Boris Shwartz talk on PhitoPsi2015 conference.
5 A. Scarpettini, D. Gomez Dumm, N.N. Scoccola, Phys. Rev. **D69**, 114018 (2004).
6 I. V. Anikin, A. E. Dorokhov and L. Tomio, Phys. Part. Nucl. **31** (2000) 509 [Fiz. Elem. Chast. Atom. Yadra **31** (2000) 1023].
7 A.E. Dorokhov, A.E. Radzhabov, A.S. Zhevlakov, Eur. Phys. J. **C71**, 1702 (2011) .
8 A.E. Dorokhov, A.E. Radzhabov, A.S. Zhevlakov, Eur. Phys. J. **C72**, 2227 (2012).
9 S. Mandelstam, Annals Phys. **19** (1962) 1.
10 J. Terning, Phys.Rev. **D44**, 887 (1991).
11 A. E. Dorokhov, A. E. Radzhabov and A. S. Zhevlakov, Eur. Phys. J. C **75** (2015) 9, 417
12 F. Jegerlehner, A. Nyffeler, Phys. Rept. **477**, 1 (2009).
13 A.E. Dorokhov, Phys. Rev. **D70**, 094011 (2004).
14 A.E. Dorokhov, Eur. Phys. J. **C42**, 309 (2005).
15 T. Goecke, C.S. Fischer, R. Williams, Phys.Rev. **D83**, 094006 (2011) [Erratum-ibid. **D86** , 099901 (2012)]; Phys.Rev. **D87**, 034013 (2013).
16 D. Greynat and E. de Rafael, JHEP **1207**, 020 (2012).
17 T. Kinoshita, B. Nizic and Y. Okamoto, Phys. Rev. D **31** (1985) 2108.